

Supplementary Materials for

A nearly complete foot from Dikika, Ethiopia and its implications for the ontogeny and function of *Australopithecus afarensis*

Jeremy M. DeSilva*, Corey M. Gill, Thomas C. Prang, Miriam A. Bredella, Zeresenay Alemseged*

*Corresponding author. Email: jeremy.m.desilva@dartmouth.edu (J.M.D.); alemseged@uchicago.edu (Z.A.)

Published 4 July 2018, *Sci. Adv.* **4**, ear7723 (2018)

DOI: 10.1126/sciadv.aar7723

The PDF file includes:

Supplementary Text

Fig. S1. The discovery of DIK-1-1f by D. Geraads on 21 January 2002 during excavation at DIK-1 locality.

Fig. S2. DIK-1-1f in various views.

Fig. S3. Talus ontogeny in apes, humans, and *A. afarensis*.

Fig. S4. Calcaneal ontogeny in apes, humans, and *A. afarensis*.

Fig. S5. Medial cuneiform ontogeny in apes, humans, and *A. afarensis*.

Fig. S6. Cuboid ontogeny in apes, humans, and *A. afarensis*.

Fig. S7. A clean section through the metatarsal shafts of the articulated DIK-1-1f shows the transverse arch of this foot.

Fig. S8. Compared to the apes, humans have proximodistally elongated cuneiforms.

Fig. S9. The calcaneus, talus, navicular, and medial cuneiform have been rearticulated in a human, chimpanzee, gorilla, DIK-1-1f, and a composite Hadar foot.

Fig. S10. Metatarsal base ontogeny in apes, humans, and *A. afarensis*.

Other Supplementary Material for this manuscript includes the following:

(available at advances.sciencemag.org/cgi/content/full/4/7/ear7723/DC1)

Data file S1 (Microsoft Excel format). Raw measurements used in this study.

Supplementary Text

Burtele and Hadar. Throughout this manuscript, we refer to the DIK-1-1f foot as a juvenile *Australopithecus afarensis*. The recent discovery, also in Ethiopia, of a contemporaneous partial foot from a hominin species with an opposable hallux (*11*) challenges the assumption that isolated fossils from the Pliocene of Eastern Africa can be unequivocally assigned to *Au. afarensis* since there is now postcranial, in addition to craniodental evidence that *Au. afarensis* shared the landscape with another partially bipedal hominin species. While there is craniodental evidence for Dikika's assignation to *Au. afarensis* (*1*) we can independently evaluate the pedal evidence that the Dikika juvenile is an *Au. afarensis*. It is important to note that by *Au. afarensis*, we specifically mean the pedal fossils from the 333 locality at Hadar, given that no pedal remains are known from the type locality at Laetoli or from any other locality at Hadar besides the A.L. 288 Lucy locality (a talus, and two pedal phalanges). Unfortunately, there are very few overlapping elements between the Dikika foot and the Burtele foot. However, the Burtele foot differs from *Au. afarensis* in having an opposable hallux and gracile, ape-like, metatarsal bases. For both of these anatomies, the Dikika foot is better aligned with the 333 pedal remains than with the Burtele specimen. While Dikika certainly had some hallucal tarsometatarsal joint mobility, it lacked the opposable hallux found in the Burtele fossil, and though none of the metatarsals are complete, the base of the fourth metatarsal in particular is dorsoplantarly taller than in similarly sized and aged apes. Compared to the mediolateral width of the proximal facet, modern humans, and material assigned to *Au. afarensis* (an undescribed second metatarsal A.L. 333-133 [fig. S10], and the fourth metatarsal A.L. 333-160 [13]) have dorsoplantarly expanded bases. In contrast, modern gorillas, chimpanzees, and the two metatarsals from the Burtele foot have dorsoplantarly truncated bases, and perhaps therefore a more mobile midfoot.



Fig. S1. The discovery of DIK-1-1f by D. Geraads on 21 January 2002 during excavation at DIK-1 locality. Projecting from the sandstone is the sheared tibial diaphysis. Photograph by Z. Alemseged.



Fig. S2. DIK-1-1f in various views. Top (left to right): dorsal with the tibia in line with the view of the camera and the foot dorsiflexed; dorsal with the dorsum of the foot in line with the camera and the tibia dorsiflexed; plantar; proximal with the focus on the tibiotalar joint; proximal with the calcaneus in focus. Bottom (left to right): medial, lateral, and distal. Scale bar is 1 cm.

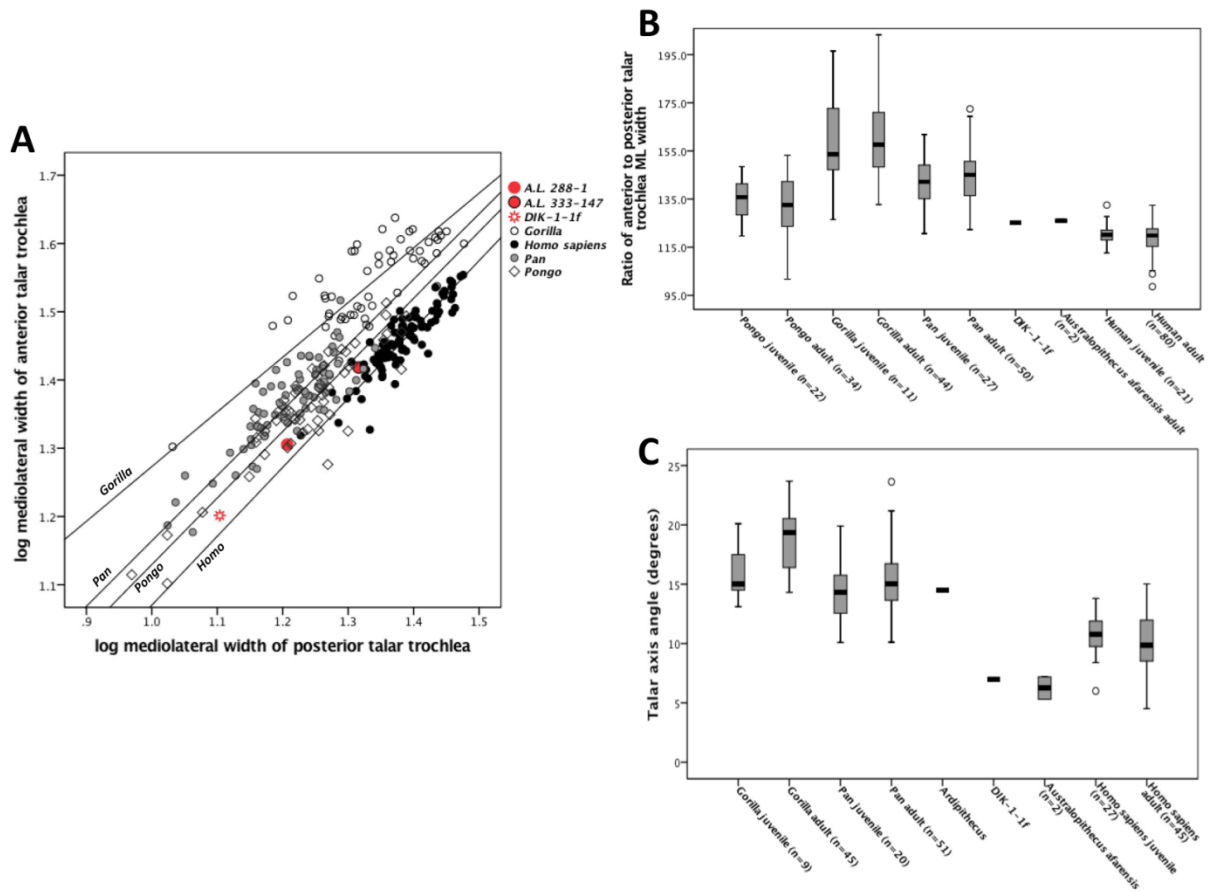
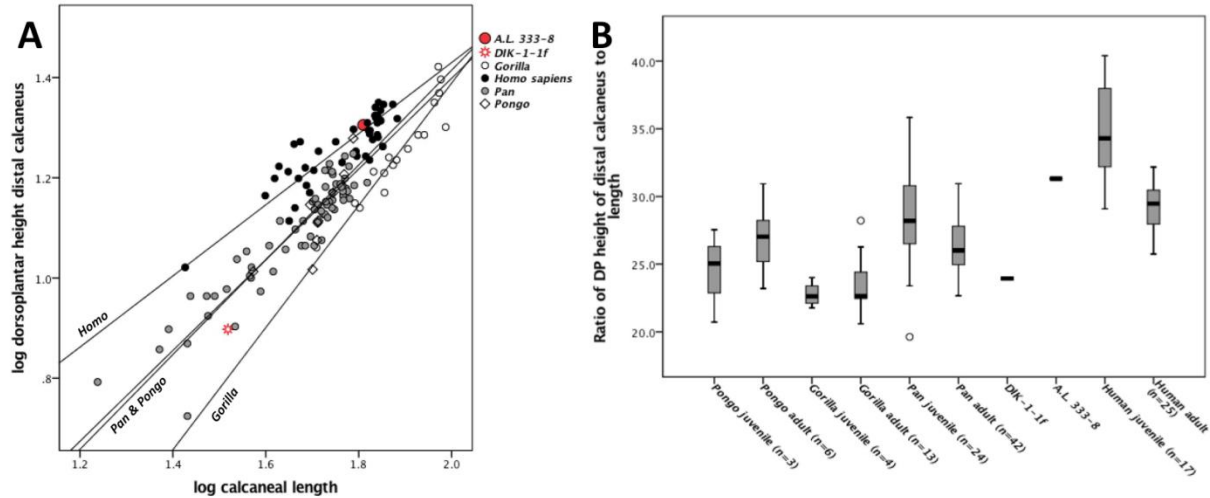


Fig. S3. Talus ontogeny in apes, humans, and *A. afarensis*. **A:** The talar trochlea of apes is more wedged (mediolateral width of anterior trochlea greater than the posterior) than the human talar trochlea. This is particularly the case for *Gorilla*. Wedging scales isometrically in humans (95% CI of slope encompasses 1). DIK-1-1f and adult *A. afarensis* (A.L. 288-1 and A.L. 333-147) are positioned between the orangutan and human RMA regression lines. RMA regression lines are drawn through the data: gorilla: $y=0.802x + 0.472$; chimpanzee: $y=0.959x + 0.206$; orangutan: $y=0.976x + 0.154$; human: $y=1.01x - 0.06$. **B:** Wedging of the talar trochlea in juvenile and adult apes and humans measured as a ratio of the mediolateral width of the anterior (distal) trochlea over the posterior (proximal) trochlear surface. Apes tend to have more wedged tali and *Au. afarensis* falls between the upper end of the human range, and lower end of the chimpanzee and orangutan range. **C:** Humans have a vertical shank relative to the ankle joint and this geometry of the lower limb is reflected in the talar axis angle (4, 38). DIK-1-1f and two adult *Au. afarensis* (A.L. 288-1 and A.L. 333-147) are on the low end of the modern human distribution, strikingly distinct from the anatomy found in the apes and *Ardipithecus* (10).



¹Values above-diagonal represent *p*-values derived from Tukey's pairwise comparisons; Bold values on the diagonal represent species averages

Fig. S4. Calcaneal ontogeny in apes, humans, and *A. afarensis*. **A:** The dorsoplantar height of the distal calcaneus is plotted against calcaneal length. Human calcanei scale with negative allometry (95% CI of slope < 1), meaning that smaller, juvenile human calcanei have proportionally taller (DP) distal calcaneal regions. DIK-1-1f is decidedly ape-like in this anatomy (see fig. 1), while the adult *Au. afarensis* specimen is human-like. RMA regression lines are drawn through the data: gorilla: $y=1.22x - 1.051$; chimpanzee: $y=0.906x - 0.413$; orangutan: $y=0.946x - 0.477$; human: $y=0.71x - 0.01$. **B:** Relative height of the distal calcaneus measured as a ratio of the dorsoplantar dimension of the distal calcaneus relative to the total bone length in juvenile and adult apes and humans. DIK-1-1f is ape-like in having a short distal calcaneus while the adult *Au. afarensis* calcaneus (A.L. 333-8) falls well within the human range. **C:** Pairwise comparisons of relative cross-sectional area of calcaneal tuber in adults and juveniles. Human juveniles and adults have more robust calcanei than the other apes. Ape adult calcanei are relatively less robust than juvenile calcanei. In *Au. afarensis*, adult calcanei are more robust. In humans, there is no statistically significant difference in robusticity between juveniles and adults.

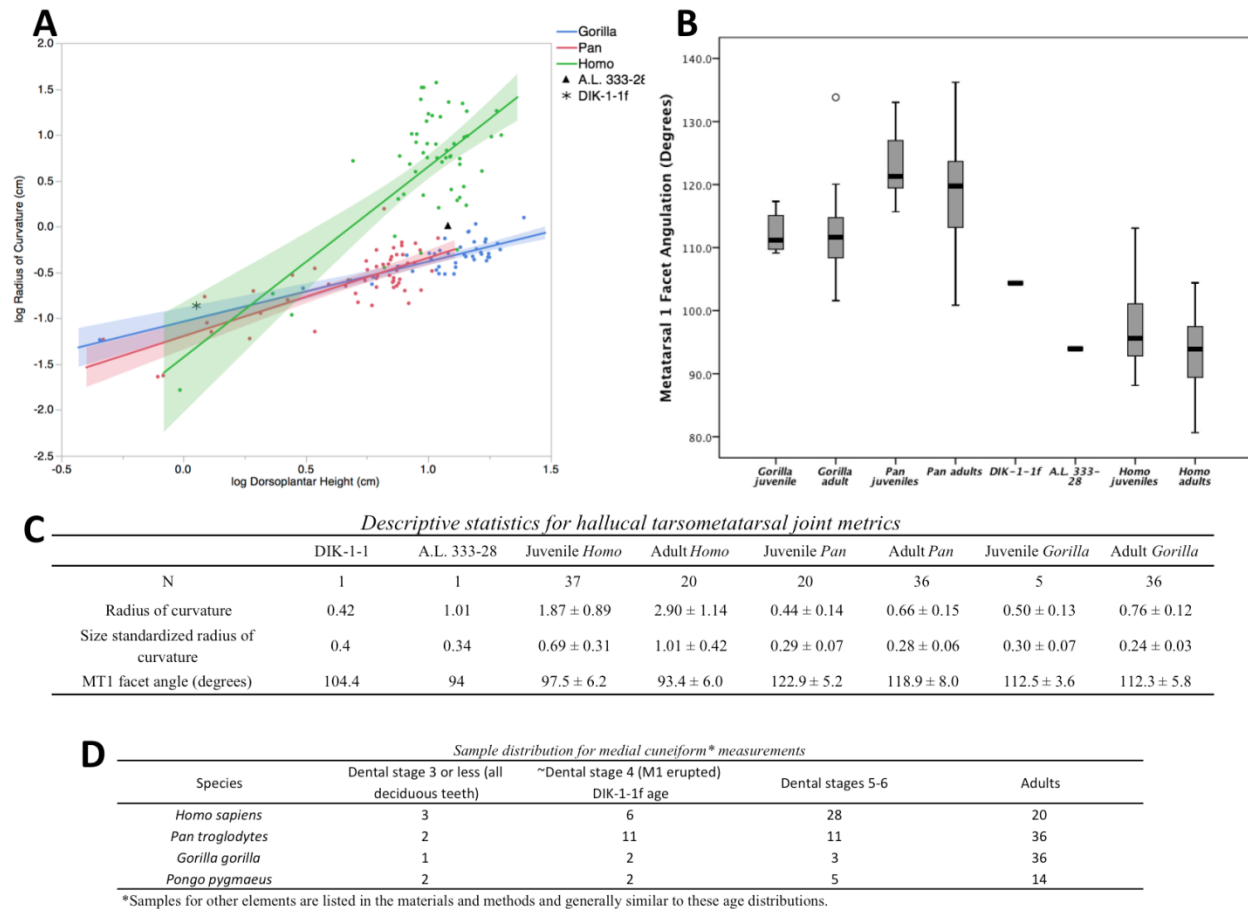


Fig. S5. Medial cuneiform ontogeny in apes, humans, and *A. afarensis*. **A:** Ontogenetic trajectory of distal facet curvature in human (green), chimpanzee (red), and gorilla (blue) medial cuneiforms. Shaded region around lines is the 95% confidence interval for the regression. The relationship between facet curvature and growth is statistically significant for all taxa (human $R^2=0.48$; gorilla $R^2=0.70$; chimpanzee $R^2=0.60$; $p<0.001$ for all). Juvenile humans and apes both possess convex distal facets and DIK-1-1f falls within the gorilla range given its size. As the medial cuneiform grows, the facet flattens abruptly in humans, but more gradually in apes (9). Although the distal facet in the adult *Au. afarensis* medial cuneiform (A.L. 333-28; triangle) is flatter than in apes, it is more convex than the morphology found in humans. The resulting line created by connecting DIK-1-1f to A.L. 333-28 parallels the ontogenetic pattern seen in apes, though we caution that only two specimens are used to generate this “slope”. **B:** Facet angulation in DIK-1-1f falls within the overlapping distribution of adult African apes and juvenile modern humans. The adult *Au. afarensis* specimen (A.L. 333-28) is distinctly human-like. These anatomies result in an adducted, but moderately mobile tarsometatarsal joint in *Au. afarensis*, a combination unknown in extant taxa. **C:** Descriptive statistics for radius of curvature and Mt1 facet angulation used in this paper. **D:** Sample distribution used in this study. Medial cuneiforms of overlapping developmental age as DIK-1-1f are in the second column.

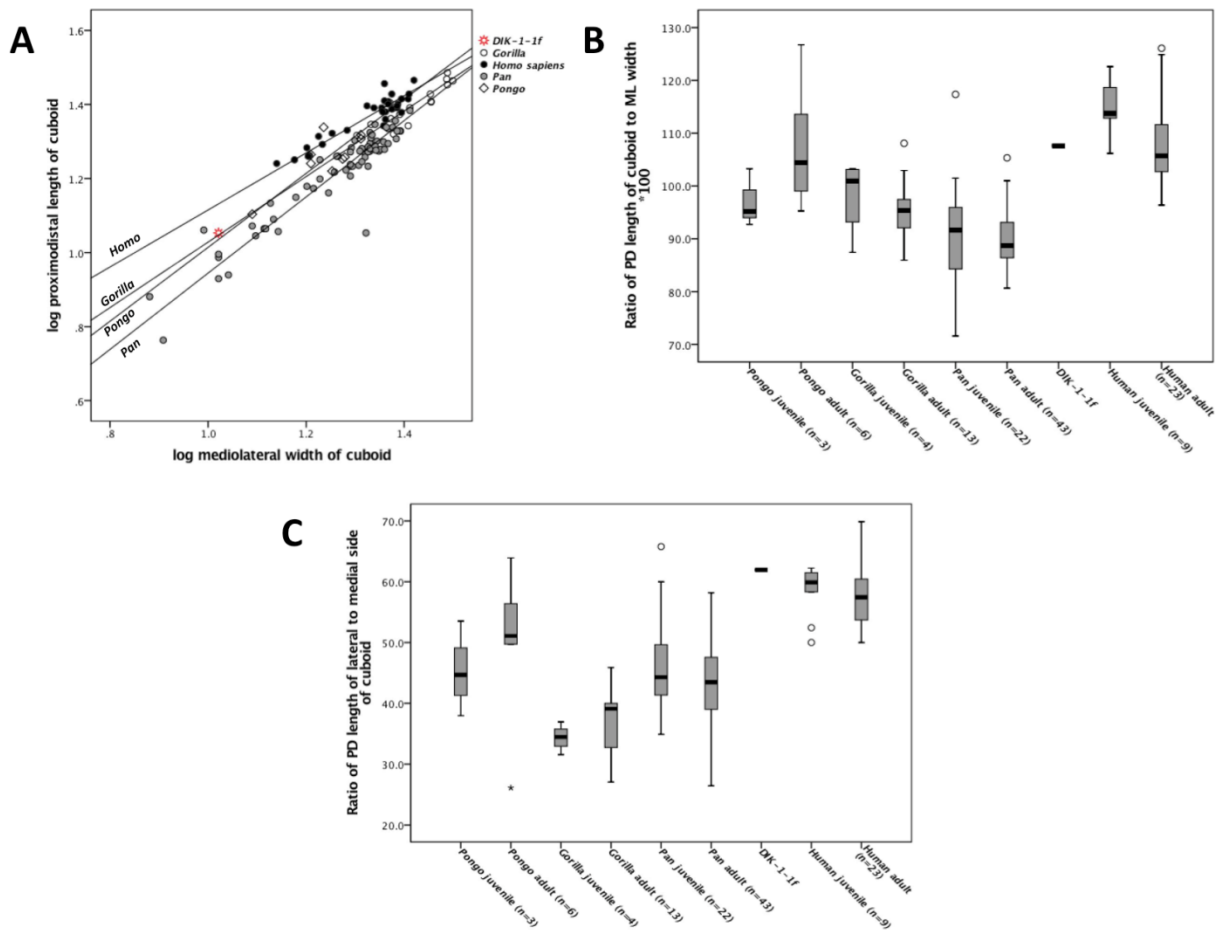


Fig. S6. Cuboid ontogeny in apes, humans, and *A. afarensis*. **A:** Human cuboids are proximodistally elongated compared to those of apes. RMA regression lines are drawn through the data: gorilla: $y=0.885x + 0.143$; chimpanzee: $y=1.03x - 0.086$; orangutan: $y=0.999x + 0.0154$; human: $y=1.10x - 0.37$, all of which are within the 95% CI of isometric scaling. **B:** Ratio of proximodistal length to mediolateral width of the cuboid in humans and apes. Notice that DIK-1-1f falls within the human distribution, distinct from the African apes in particular. The elongated cuboid may represent the primitive condition, with African apes independently shortening the cuboid (10). **C:** The ratio of the proximodistal length of the medial and lateral edges of the cuboid are plotted here and demonstrate that humans have laterally elongated edges relative to the medial length of the cuboid. DIK-1-1f shares this human-like anatomy. African apes, in contrast, have PD foreshortened lateral edges, resulting in a lateral tapering of the cuboid.

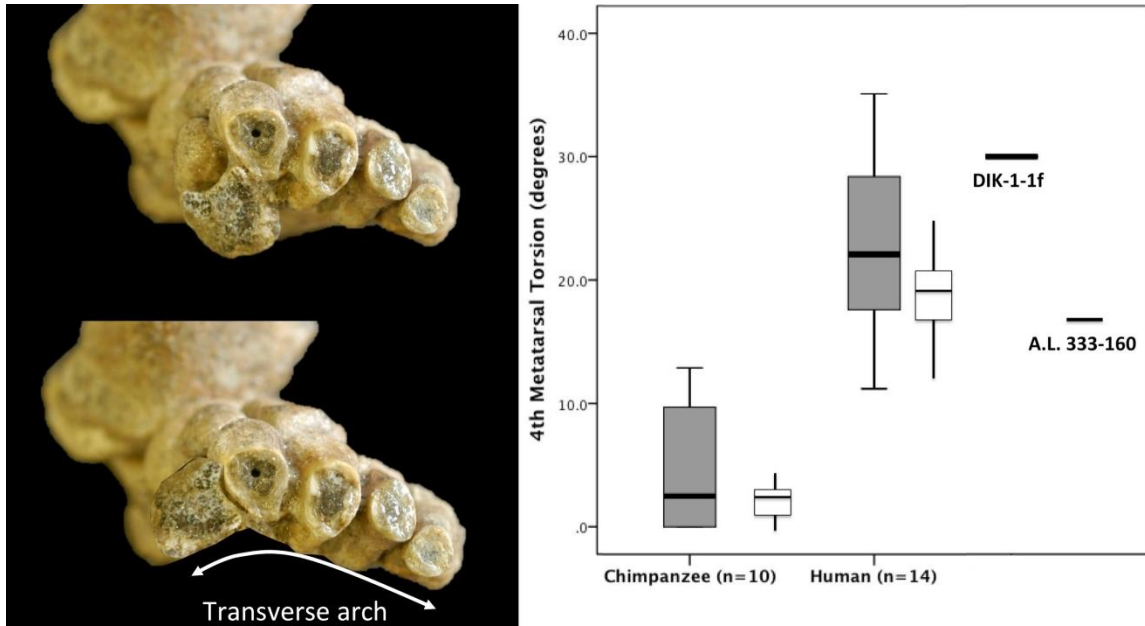


Fig. S7. A clean section through the metatarsal shafts of the articulated DIK-1-1f shows the transverse arch of this foot. Though the bones remain in near anatomical position, there has been some slight shifting. The fifth metatarsal has rotated externally so that the fourth metatarsal facet faces plantarly and the epiphysis of the first metatarsal has internally rotated so that the horseshoe shaped contact with the second metatarsal faces dorsally. When the epiphysis is repositioned (bottom image, but note: the fifth metatarsal position is not repositioned), the transverse arch of the foot is apparent. However, the arch is probably not as elevated—especially medially—as in modern human children (Fig. S9). To the right, the torsion of the fourth metatarsal in human and chimpanzee juveniles (dark gray boxplots) are shown with adult data (white boxplots redrawn from ref. 13), and plotted with A.L. 333-160 and the estimated torsion of the fourth metatarsal based on the externally rotated shaft of DIK-1-1f. These data indicate that juvenile humans already possess externally torqued metatarsal shafts and while we stress caution in directly comparing shaft torsion (DIK-1-1f) with torsion measured at the epiphyseal surface (data shown in the gray boxplots), DIK-1-1f undoubtedly presents an externally torqued fourth metatarsal shaft, as is found in adult *Au. afarensis* (13).

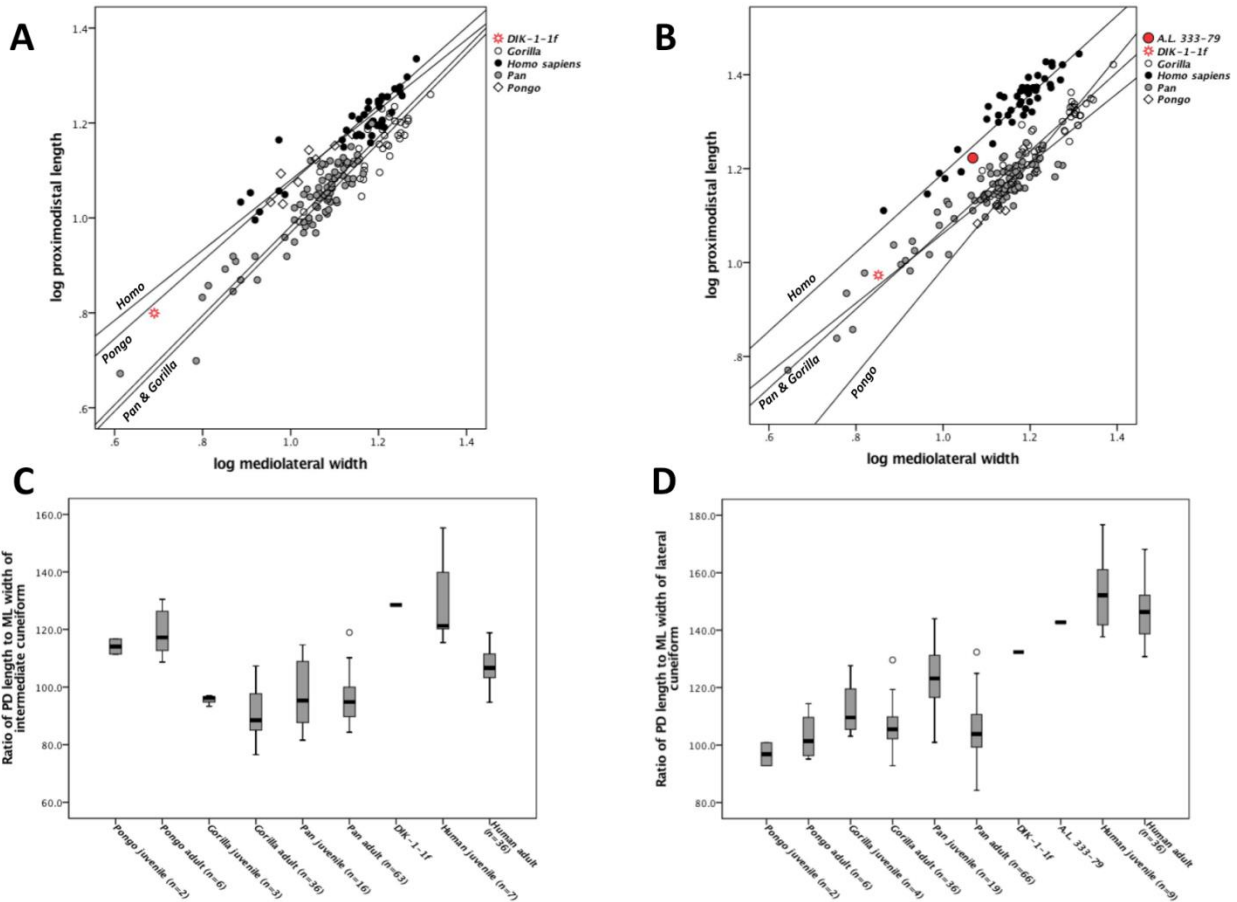


Fig. S8. Compared to the apes, humans have proximodistally elongated cuneiforms. A: Intermediate cuneiform proximodistal elongation is examined ontogenetically in humans and apes. The intermediate PD elongation scales with negative allometry in both humans and with isometry in the African apes. RMA regression lines are drawn through the intermediate cuneiform data: gorilla: $y=0.942x + 0.027$; chimpanzee: $y=0.940x + 0.042$; orangutan: $y=0.820x + 0.253$; human: $y=0.74x + 0.34$. **C:** Based on the ratio of PD length to ML width in juvenile and adult apes and humans, DIK-1-1f is elongated relative to juvenile apes and falls within the human range, though orangutans also possess a PD elongated intermediate cuneiform. **B:** The proximodistal length of the lateral cuneiform is plotted against the mediolateral width of the bone. Humans and African apes scale with negative allometry (95% CI of slopes <1), meaning that the bone becomes less elongated as it enlarges mediolaterally. RMA regression lines are drawn through the data: gorilla: $y=0.841x + 0.228$; chimpanzee: $y=0.744x + 0.318$; orangutan: $y=1.13x - 0.139$; human: $y=0.84x + 0.35$. **D:** The ratio of PD length to ML width in juvenile and adult apes and humans reveals that adult *Au. afarensis* (A.L. 333-79) is human-like, while DIK-1-1f is outside the human juvenile range and nearer to chimpanzee juveniles in being PD foreshortened.

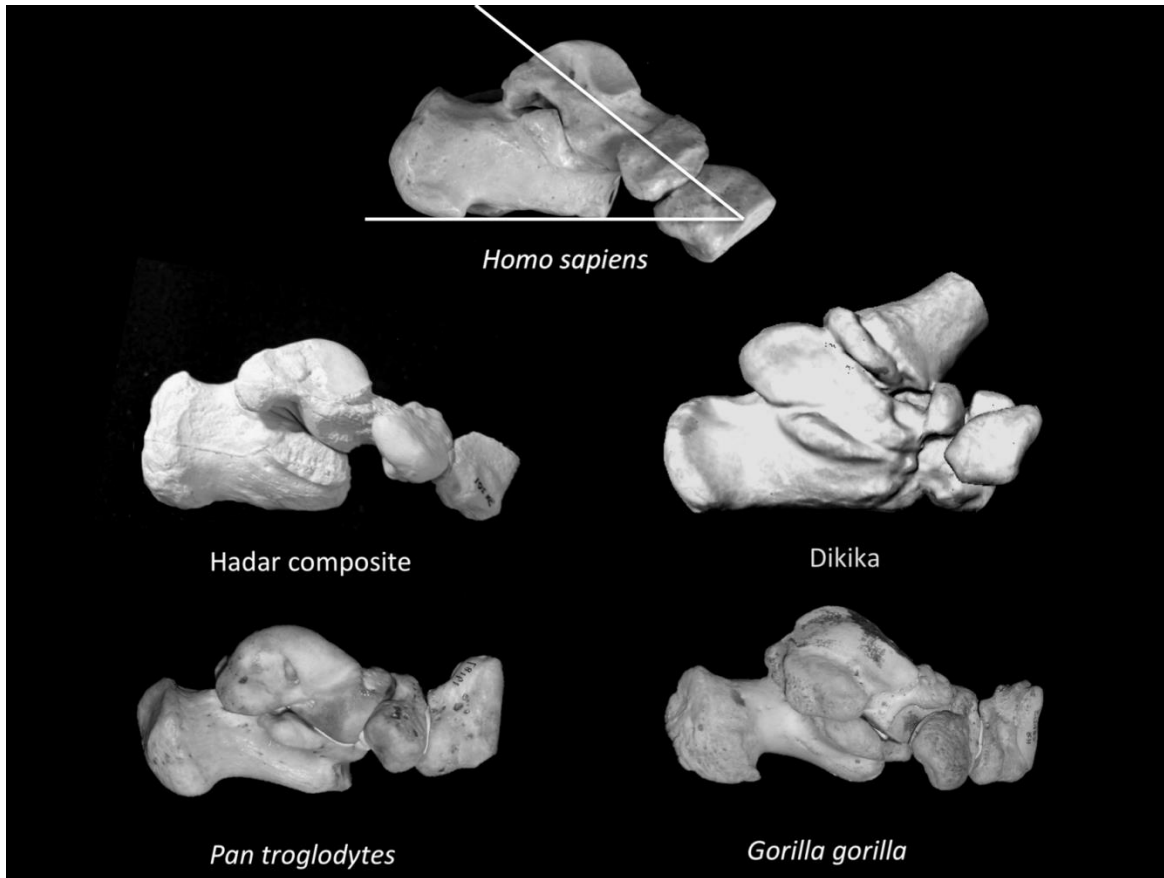


Fig. S9. The calcaneus, talus, navicular, and medial cuneiform have been rearticulated in a human, chimpanzee, gorilla, DIK-1-1f, and a composite Hadar foot. The feet have been scaled to roughly the same size and oriented so that the talar trochlea is parallel in the coronal plane, and the plantar aspect of the calcaneus is level (not inclined). The Hadar composite right foot consists of casts of A.L. 333-8 (calcaneus), A.L. 333-147 (talus), A.L. 333-36 (navicular), and A.L. 333-28 (medial cuneiform). The calcaneus and talus are not from the same individual (though a mirrored A.L. 333-147 talus articulates well with the A.L. 333-55 calcaneus); however, the articulating surfaces of A.L. 333-36 and A.L. 333-28 are congruent and have similar patinas suggesting they may be from the same individual. With these bones, a talocalcaneal angle (illustrated for the human) can be estimated. The human is $\sim 40^\circ$, near the mean in humans measured from radiographs (18). Chimpanzees and gorillas ($n=7$) measure 16.6° (range 13.6° - 20.1°), though a talocalcaneal angle is difficult to take on apes given that the medial cuneiform deflects dorsally since the navicular tuberosity may contact the substrate. In the Hadar composite, the talocalcaneal angle is $\sim 25^\circ$, while the same measurement is $\sim 20^\circ$ in DIK-1-1f, though this should be regarded as an estimate since the navicular has shifted dorsally and the talus is plantarflexed and everted at the subtalar joint. Given that shifting of individual elements may make this observation speculative, we estimated the talar declination angle on the DIK-1-1f to $\sim 20^\circ$, similar to that found in A.L. 288-1 and African apes, but quite low for modern humans (16). A recent CT study has found that low talar declination angles are found in modern human feet with *pes planus* (17). We interpret these morphologies collectively as evidence that the *Australopithecus* foot was slightly arched relative to an ape foot, but far lower than the average modern human arch.

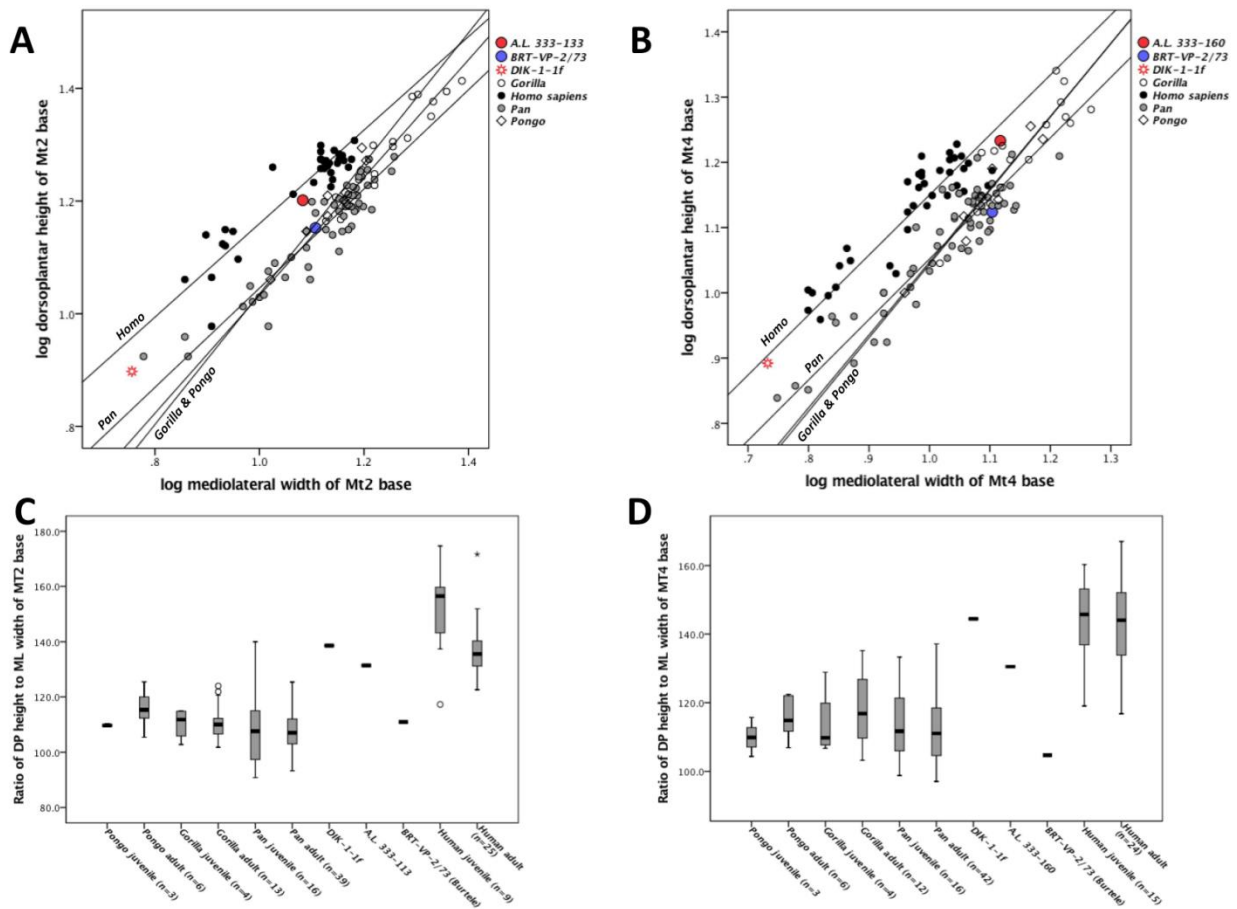


Fig. S10. Metatarsal base ontogeny in apes, humans, and *A. afarensis*. **A&B:** The dorsoplantar height of the second (left) and fourth (right) metatarsal bases are plotted against the mediolateral width of the metatarsal base in apes and humans. In juveniles and adults alike, the human metatarsal base is consistently DP taller than the ML width with isometric scaling in all cases except the human second metatarsal, which scales with slight negative allometry. RMA regression lines are drawn through the second metatarsal data—gorilla: $y=1.05x - 0.014$; chimpanzee: $y=0.881x + 0.165$; orangutan: $y=1.16x - 0.124$; human: $y=0.83x + 0.33$. RMA regression lines are drawn through the fourth metatarsal data—gorilla: $y=0.928x + 0.124$; chimpanzee: $y=1.12x - 0.070$; orangutan: $y=1.13x - 0.084$; human: $y=0.92x + 0.23$. **C&D:** Ratios of DP height to ML width of the bases of metatarsals 2 and 4 are presented for juvenile and adult apes and humans. DIK-1-1f is human-like in DP height for its size, while the undescribed second metatarsal from Hadar (A.L. 333-133) is also human-like. The Burtele second metatarsal is quite ape-like. Both DIK-1-1f and the adult fourth metatarsal (A.L. 333-160) possess human-like, DP tall bases. The Burtele fourth metatarsal clusters with the apes.